Fatigue Fracture of Neat and Short Glass Fiber Reinforced Polypropylene: Effect of Frequency and Material Orientation

ALESSANDRO PEGORETTI[1] AND THEONIS RICCO
Department of Materials Engineering
University of Trento
Via Mesiano 77
38050 Trento, Italy

(Received November 12, 1998)
(Revised July 14, 1999)

ABSTRACT: The influence of glass fibers content and testing conditions (frequency and mean load) on the fatigue crack propagation rate in injection molded neat and fiber reinforced polypropylene has been investigated. The resistance to fatigue crack propagation increases as the fiber volume fraction increases. The fatigue resistance of either neat and fiber reinforced polypropylene is tremendously dependent on the crack propagation direction, with higher values for crack propagating transversely to the melt flow direction in the molded plaques. A dramatic increase of the crack growth rate per cycle by decreasing frequency, at any given crack length was found for all the materials investigated. Analysis of data obtained at various frequencies and applied mean loads suggests that crack propagation is determined mostly by viscoelastic creep processes at the crack tip, the role of pure fatigue appearing quite secondary.

KEY WORDS: mechanical properties, fatigue, short-fiber composites, glass fibers, polypropylene matrix.

INTRODUCTION

ISOTACTIC POLYPROPYLENE (PP) REPRESENTS one of the most interesting large-volume thermoplastics with wide application in the automotive [1], appliances, and house-hold fields. PP is characterized by many interesting properties such as low density, relative high thermal stability, good processability and resistance to degradation. When proper fillers and/or reinforcements are incorporated

[1]Author to whom correspondence should be addressed.

1530-793X/00/12 1009–19 $10.00/0 DOI: 10.1106/KF4C-438N-JFHB-H3EB

into PP, stiffness, strength and damage tolerance can be enhanced to fulfill the gap between commodities and engineering thermoplastics [2].

The strong focus on load-bearing industrial applications leads to a particular attention toward the fracture behavior of injection molded neat and filled PP components. In particular, the fatigue properties are of paramount importance for many intended applications where components are subjected to load and environmental histories which vary in time over the period of service [2–10]. Fatigue damage is associated with the initiation and propagation of cracks in the matrix and/or the destruction of the bonding at the fiber/matrix interface. Final failure of PP and its short-fiber reinforced (SFR) composites under alternating loadings, mainly occurs by fatigue crack propagation (FCP) [2,5,6,10] characterized by a stable crack acceleration range which can be reasonably well described by the Paris-Erdogan relationship [11]:

$$\frac{da}{dN} = A\Delta K^n \tag{1}$$

where da/dN is the crack growth per each cycle, A and n are constants and ΔK is the stress intensity amplitude at the crack tip under mode I (opening mode). In general, the most important testing variables affecting the FCP rate are frequency and wave form of the alternating load, temperature, environment, stress ratio and mean load [5]. Moreover material variables such as molecular weight, crystallinity, fiber content and orientation also play a major role in determining the FCP behavior [2].

In processing operations, such as extrusion or injection molding, the hydrodynamic force field generated by the flow always produces some degree of orientation depending on the tool design [12]. Such orientation phenomena are responsible for anisotropic mechanical properties due to macromolecules partial alignment and/or, in the case of SFR composites, due to fiber preferred orientation. The effect of fiber partial alignment on the FCP behavior of SFR composites has been examined by a number of authors on several kinds of thermoplastic matrices such as polypropylene [2,5], polyamide [13–19], polyethylene [20], polyetheretherketone [21,22], polybutylenterephthalate [23], polyethersulphone [24], and polytetrafluoroethylene [25]. In all cases the FCP resistance results to be enhanced by the presence of fibers, particularly when they are preferentially aligned transversely to the crack growth direction.

The aim of the present paper is to investigate the effect of fiber volume fraction, fiber orientation, mean load and test frequency on the FCP rate in polypropylene short glass fiber reinforced composites.

EXPERIMENTAL

Unfilled PP (Moplen 7073 XOP) and its short glass fiber composites reinforced with 10, 20, and 30 weight % (i.e., 3.9, 8.3, and 13.5 volume %) were supplied by

Montell Polyolefins S.p.A. (Ferrara, Italy) in the form of injection molded square plaques (see Figure 1) with $L = 127$ mm and $B = 2.5$ mm. The fiber volume fractions (V_f) were evaluated for each composite from the matrix and fiber weight fractions (W_f) assuming the densities of glass fibers and matrix of 2.50 and 0.91 kg m^{-3}, respectively. All plaques were obtained using a Negri-Bossi NB90 injection-molding machine under the following conditions:

- melt temperature = 285°C
- injection pressure = 4.5 MPa
- holding pressure = 4.5 MPa
- mold filling time = 12.5 s
- holding time = 30 s
- cooling time = 60 s

The short E-glass fibers (Owens Corning R34B), with an average initial length of 4.5 mm and a diameter, d, of 14 μm, were treated with a polypropylene compatible coating (Hercoprime HG 201). After compounding and injection molding, the manufacturer evaluated an average fiber length, l, in the molded plaques of about 400 μm, i.e., an average fiber aspect ratio, l/d, of about 30.

A differential scanning calorimeter Mettler DSC 30 was used to detect the melting temperature, T_m, and the crystallinity content, X_c, of the matrix by integrating the normalized area of the endothermal peak and rating the heat involved to the ref-

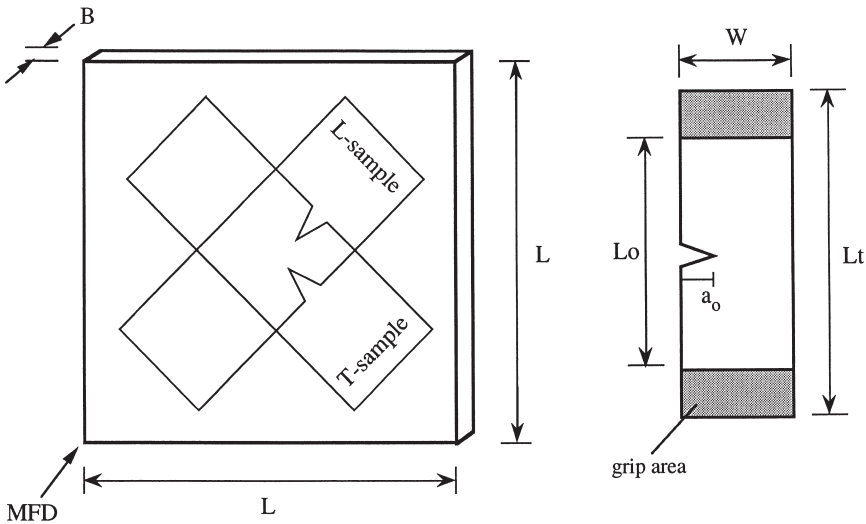

Figure 1. *Geometry of the injection molded plaques, and positions of L and T-samples machined from them. MFD indicates the mold filling direction.*

erence value of the 100% crystalline polymer (210 J/g) [26]. The conditions for DSC measurements were as follows: specimen weight: about 20 mg; temperature interval: 0 to 230°C; heating rate: 10°C/min; nitrogen flux: 100 ml/min.

Monotonic uniaxial tensile tests were performed on rectangular unnotched specimens of $10 \times 120 \times 2.5$ mm^3 with an Instron 4502 tensile tester equipped with a 10 kN load cell by using a strain gauge extensometer (Instron, model 2620). All measurements were performed at room temperature, at a cross-head speed of 10 mm min^{-1} on at least 5 specimens. Samples were machined both longitudinally (L-samples) and transversely (T-samples) with respect to the mold-fill direction, as depicted in Figure 1.

Toughness measurements were performed following the procedure indicated in the ASTM standard D 5045 [27]. Single-edge notch bending (SENB) specimens were obtained along longitudinal (L-samples) or transverse (T-samples) direction, as depicted in Figure 1. The specimen dimensions were $8 \times 60 \times 2.5$ mm^3, the span was 32 mm and the initial notch length was 4 mm. The specimens were loaded by using an Instron 4502 machine at a cross-head speed of 10 mm min^{-1} (low speed test, nominal strain rate of 0.008 s^{-1}). Fracture toughness measurements at higher speed were performed on the same type of specimens by using an instrumented Charpy pendulum (CEAST S.p.A., Torino, Italy) with an impact speed of 0.925 m s^{-1} (high speed test, nominal strain rate of 43.4 s^{-1}). Due to the specimens' thinness, the size requirements for the K_{IC} determination were not completely satisfied. The guideline regarding the linearity recommendation was satisfied in all cases except for the pure PP matrix. In both cases (low or high speed), apparent fracture toughness, K_c^*, values were calculated using the following formula [27]:

$$K_c^* = \frac{F_c}{BW^{1/2}} f\left(\frac{a}{W}\right) \tag{2}$$

where

$$f\left(\frac{a}{W}\right) = 6\left(\frac{a}{W}\right)^{1/2} \frac{\left[1.99 - \left(\frac{a}{W}\right)\left[1 - \left(\frac{a}{W}\right)\right]\left[2.15 - 3.93\left(\frac{a}{W}\right) + 2.7\left(\frac{a}{W}\right)^2\right]\right]}{\left[1 + 2\left(\frac{a}{W}\right)\right]\left[1 - \left(\frac{a}{W}\right)\right]^{3/2}} \tag{3}$$

F_c is the maximum load measured either in the low or high speed tests, B is the specimen thickness, W is the specimen width, and $x = a/W$ where a is the initial crack length.

Fatigue crack propagation experiments were carried out on single-edge notch tension (SENT) L and T samples whose positions in the original injection molded square plaques are reported in Figure 1. The specimens' dimensions were chosen in accordance to the ISO/TC 61/SC 2/WG 7 N5 recommendations,

i.e., $B = 2.5$ mm, $W = 27$ mm, $L_t = 140$ mm, and $L_0 = 60$ mm. An initial crack of length $a_0 = 3$ mm was made by means of a razor blade. All the fatigue tests were performed with a closed loop servohydraulic MTS 858 Mini Bionix testing machine, at room temperature, under tension-tension sinusoidal load control. The cyclic frequencies were 0.1, 1, and 10 Hz, the mean load was 1200 N with a minimum to maximum load ratio of 0.4, except for the experiments where the effects of the mean load was examined. Using a video camera, a video-recorder, and an image analyzer system, the crack length, a, was monitored as a function of the number of cycles, N, without test interruption. For each experimental situation, at least three separate specimens were tested and an average crack propagation rate was obtained as the derivative of the best fitting polynomial curve. The stress intensity factor, K, at the crack tip was evaluated on the basis of the linear elastic fracture mechanics approach which is often used to also describe fracture and fatigue behavior of nonlinear elastic and heterogeneous materials [3]. The specific equation for the stress intensity factor amplitude, ΔK, for SENT specimens is [28]:

$$\Delta K = \frac{\Delta P}{BW}\sqrt{a}Y\left(\frac{a}{W}\right) \tag{4}$$

where

$$Y\left(\frac{a}{W}\right) = \left[1.99 - 0.41\frac{a}{W} + 18.7\left(\frac{a}{W}\right)^2 - 38.48\left(\frac{a}{W}\right)^3 + 53.85\left(\frac{a}{W}\right)^4\right] \tag{5}$$

ΔP is the difference between the maximum and the minimum applied load, B is the thickness, and W the width of the specimens.

RESULTS AND DISCUSSION

Material Properties

As indicated by the DSC measurements reported in Table 1, the presence of fibers does not significantly affect the crystallinity content of the materials, while the melting temperature is slightly higher for the pure PP matrix with respect to the composites.

Table 1. Melting temperature, T_m, and crystallinity content, X_c, as measured by DSC.

Material	T_m (°C)	X_c (wt%)
PP matrix	171	43
PP + 3.9 vol% glass fibers	166	42
PP + 8.3 vol% glass fibers	166	43
PP + 13.5 vol% glass fibers	167	45

The results of static tensile tests performed on samples obtained both longitudinally (L-samples) and transversely (T-samples) to the mold fill direction are reported in Table 2. From the tensile modulus and yield strength values it comes out that the mechanical response is clearly anisotropic with higher values along the longitudinal direction, especially for fiber volume fractions higher than 3.9 vol%. In Figure 2 it is interesting to compare the experimental tensile modulus values with the theoretical previsions based on the empirical equation for the modulus, E_R, of a composite containing fibers randomly oriented in a plane [29]:

$$E_R = \frac{3}{8}E_{LL} + \frac{5}{8}E_{TT} \tag{6}$$

where E_{LL} and E_{TT} are respectively the longitudinal and transverse tensile moduli for a unidirectionally aligned short fiber composite having the same fiber aspect ratio and fiber volume fraction as the composite under consideration. Moduli E_{LL} and E_{TT} can be estimated by the well-known Halpin-Tsai micromechanics equations [30], i.e.:

$$E_{LL} = E_m \frac{1 + \zeta_L \eta_L V_f}{1 - \eta_L V_f}; \quad E_{TT} = E_m \frac{1 + \zeta_T \eta_T V_f}{1 - \eta_T V_f}$$

where E_m is the matrix modulus, V_f is the fiber volume fraction, and:

$$\zeta_L = 2\frac{1}{d}, \quad \zeta_T = 2; \quad \eta_L = \frac{\frac{E_f}{E_m} - 1}{\frac{E_f}{E_m} + \zeta_L}; \quad \eta_T = \frac{\frac{E_f}{E_m} - 1}{\frac{E_f}{E_m} + \zeta_T}$$

From Figure 2 it can be clearly observed that the measured values of the elastic modulus deviate from the theoretical prediction for composites with a random fiber distribution. In particular L-samples have a higher elastic modulus which indicates a longitudinal preferred fiber orientation, while T-samples display a lower

Table 2. Elastic moduli, E, and yield strength, σ_y, as measured in tensile tests. Subscripts L and T refer to longitudinal and transversal direction, respectively (see Figure 1).

Material	E_L (GPa)	E_T (GPa)	σ_{yL} (MPa)	σ_{yT} (MPa)
PP matrix	2.2	2.2	34.2	33.1
PP + 3.9 vol% glass fibers	3.0	2.8	51.3	40.2
PP + 8.3 vol% glass fibers	4.1	3.7	56.8*	47.6*
PP + 13.5 vol% glass fibers	5.6	4.4	63.1*	52.2*

*Taken as the maximum stress.

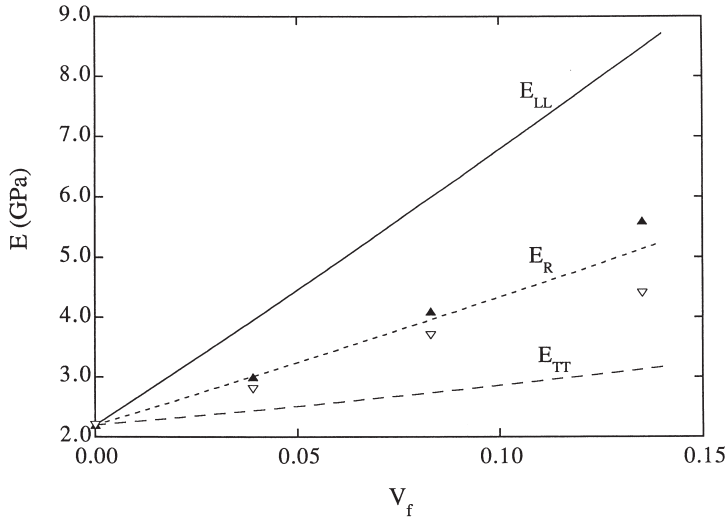

Figure 2. *Experimental values of the longitudinal (▲) and transverse (▽) elastic modulus as a function of the fiber volume fraction,* V_f*. Theoretical curves for a longitudinally,* E_{LL}*, and transversely,* E_{TT}*, perfectly aligned, or in-plane randomly distributed,* E_R*, composites are also reported.*

modulus which indicates a transverse preferred fiber orientation. It is worth noting that the difference between the longitudinal and transverse modulus increases as the fiber volume fraction increases. Nevertheless the low deviation from the theoretical modulus prediction for the case of a random fiber distribution suggests a low degree of fiber orientation even for the higher fiber content.

It is well known [31] that injection molding of short fiber reinforced thermoplastics may cause different fiber orientation across the thickness of the specimens. The surface or skin layers are usually characterized by fibers aligned predominantly parallel to the mold filling direction (MFD), while in the central or core layer the fibers are preferentially oriented transversely to the MFD. For polypropylene-SGF reinforced injection molded plaques of about 3 mm thickness, Karger-Kocsis [5] reported that the core layer is much thinner than the skin layers at all volume fractions. Even if we could not perform a complete and exhaustive fiber distribution experimental analysis, a microscopic observation of the fracture surface evidenced a very limited core structure. On the basis of the above considerations we can therefore suppose that the L-samples contain more fibers which are oriented mostly longitudinally to the load direction while the T-samples contain more fibers which are preferentially oriented transversely to the load direction.

Studies conducted on several short-fiber reinforced thermoplastics indicate that the fracture toughness can be affected in very different ways by the presence of fibrous reinforcement. In fact it has been reported that as the fiber volume fraction

increases the fracture toughness can either increase, like in the case of SGF reinforced PES [24], or remain constant, as for SGF reinforced PEEK [21], or even decrease, like for SGF reinforced PTFE [25]. Results of the fracture toughness measurements are reported in Figure 3 for the materials under investigation. It can be noticed that the addition of fibers enhances the apparent fracture toughness, K_c^* at higher values for the L-samples where the fibers are preferentially aligned transversely to the crack propagation direction. In other words in T-samples, where the fibers are mostly aligned along the crack propagation direction, fracture propagates at lower K_c^* values. Moreover the apparent fracture toughness values obtained at high testing speed are systemically lower than those obtained at lower speed. A similar rate effect has been reported [32] for PP homopolymers filled with glass flake.

Fatigue Crack Propagation (FCP)

A characteristic curve of the crack growth, Δa, vs. the number of fatigue cycles, N is reported in Figure 4(a), while in Figure 4(b) the corresponding curve of the crack propagation rate, da/dN, vs. the stress intensity factor amplitude, ΔK, can be observed. In the first stage of the fatigue test the FCP rate decreases as already observed in previous works [2,5,10] for both neat and short glass fiber reinforced

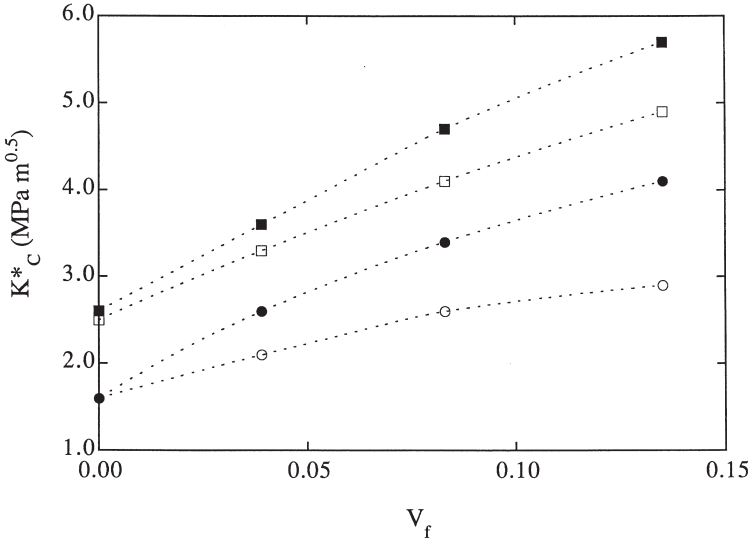

Figure 3. *Apparent fracture toughness, K_c^*, values as a function of the fiber volume fraction, V_f, as determined in low and high speed tests. Symbols as follows: (■) L direction, low speed test; (□) T direction, low speed test; (●) L direction, high speed test and (○) T direction, high speed test.*

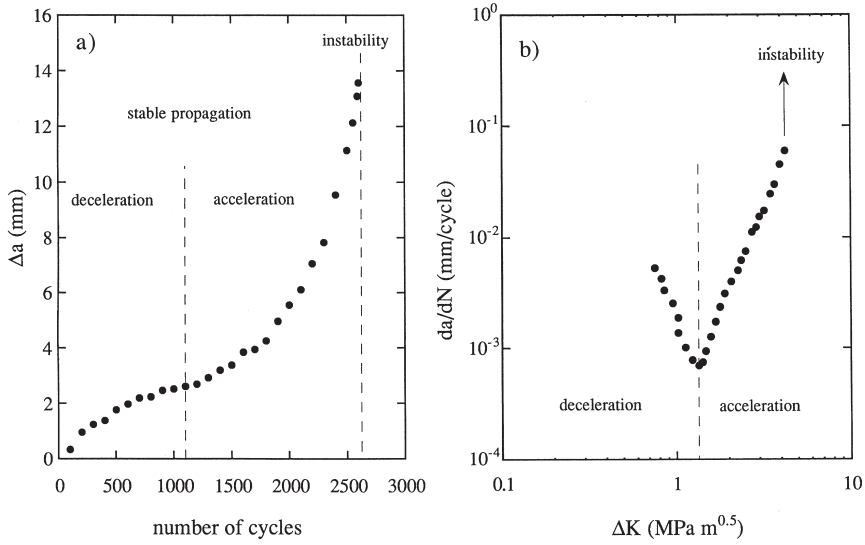

Figure 4. *Examples of typical (a) crack growth curve as a function of number of cycles and (b) crack growth rate curve as a function of the applied stress intensity amplitude.*

polypropylene. The FCP rate decreases, probably as a consequence of notch tip blunting, until a minimum value is reached, which corresponds to the onset of a stable FCP acceleration region. This region can be reasonably described by the well-known Paris-Erdogan power law [Equation (1)] up to instability and complete fracture.

EFFECT OF FIBER CONTENT AND ORIENTATION

The fatigue propagation data in the stable acceleration range obtained at a frequency of 1 Hz, for L- and T-samples with various fiber volume fractions are reported in Figure 5. From this experimental data it can be noticed that an increase of the fiber volume fraction is effective in hindering the fatigue crack growth. This effect has been reported by a number of authors for several different short glass or carbon fiber reinforced polymers like polypropylene [2,5–8,10], polyamides [14,15,18], polybutyleneterephthalate [23], polyetheretherketone [21,22], polyethersulphone [24], polytetrafluoroethylene [25]. Moreover from Figure 5 it can be observed that for both neat and fiber reinforced polypropylene, the FCP rate strongly depends on the crack propagation direction. In particular the FCP resistance is much higher in the case of L-samples with respect to T-samples. The same behavior has been previously reported on polypropylene based composites [5–7] and other short glass fiber thermoplastics like polyamides [14–19], polyetheretherketone [21,22], polyethersulphone [24], polyethylene [33].

For all the materials under investigation, the values of the constant *A* which appears in Equation (1), measured on both L- and T-samples, are reported in Figures 6, 7 and 8 as a function of the fiber volume fraction, low-rate apparent fracture toughness, and yield strength, respectively. Figure 6 clearly shows that as the fiber volume fraction increases the pre-exponential factor *A* decreases, thus confirming the observations reported by Karger-Kocsis for similar materials [5]. Moreover the FCP behavior of the L-samples is characterized by lower values of *A* than the corresponding T-samples. Similar observations hold for Figure 7 which shows how coefficient *A* is decreasing as the fracture toughness increases. It is worth noting that the markedly different FCP behavior between L- and T-samples cannot be explained only on the basis on their apparent fracture toughness values. In other words, samples with similar fracture toughness exhibit strongly different FCP rates for a given ΔK. From Figure 8 it is evident that for the composite under investigation the pre-exponential factor *A* linearly decreases as the tensile yield strength increases. From the above considerations it seems reasonable to hypothesize that the fatigue crack propagation in SGF reinforced PP involves deformation mechanisms responsible for the yielding processes at the crack tip. The data reported in Figure 8 are further indicating that the FCP process in pure PP matrix is characterized by *A* values lower that those attainable by linearly extrapolating the data of the composites, thus suggesting different fracture mechanisms.

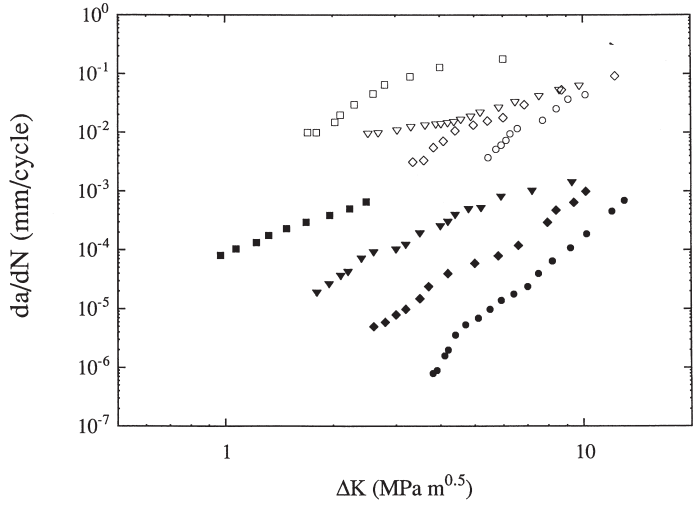

Figure 5. da/dN *vs* ΔK *plots, in a double logarithmic scale, obtained at a mean load of 1200 N, frequency 1 Hz, minimum to maximum load ratio* R = *0.4. Symbols as follows: (■)* L *direction,* V_f = *0 vol%; (▼)* L *direction,* V_f = *3.9 vol%; (◆)* L *direction,* V_f = *8.3 vol%; (●)* L *direction,* V_f = *13.5 vol%; (□)* L *direction,* V_f = *0 vol%; (▽)* L *direction,* V_f = *3.9 vol%; (◇)* T *direction,* V_f = *8.3 vol%; (○)* T *direction,* V_f = *13.5 vol%.*

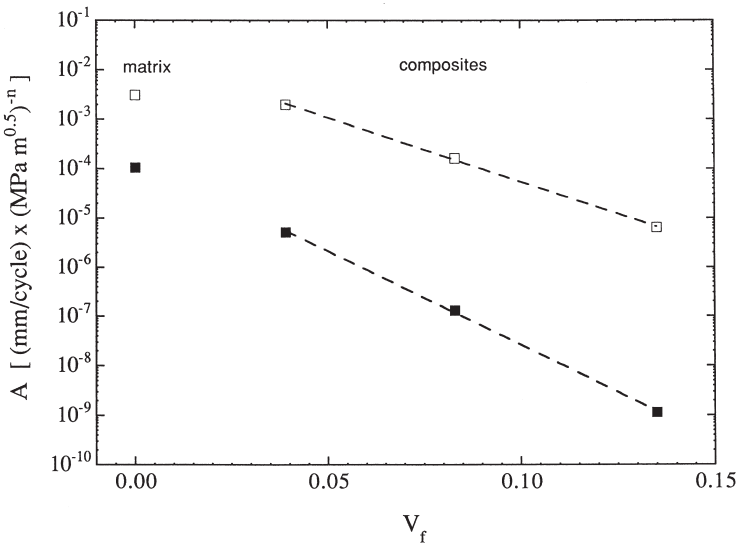

Figure 6. *Pre-exponential* A *coefficient of the Paris-Erdogan equation as a function of the fiber volume fraction for tests performed at a mean load of 1200 N, frequency 1 Hz, minimum to maximum load ratio* R = *0.4. Symbols as follows: (■)* L *direction and (□)* T *direction.*

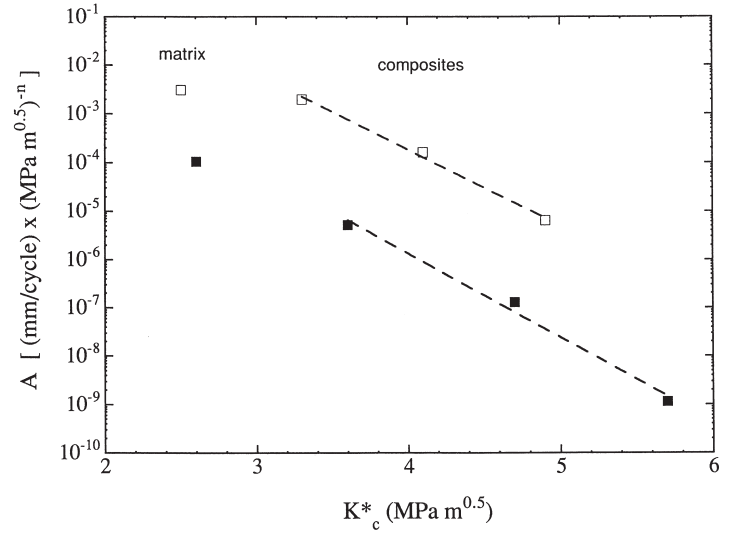

Figure 7. *Pre-exponential* A *coefficient of the Paris-Erdogan equation as a function of low-rate apparent fracture toughness,* K_c^*, *for fatigue tests performed at a mean load of 1200 N, frequency 1 Hz, minimum to maximum load ratio* R = *0.4. Symbols as follows: (■)* L *direction and (□)* T *direction.*

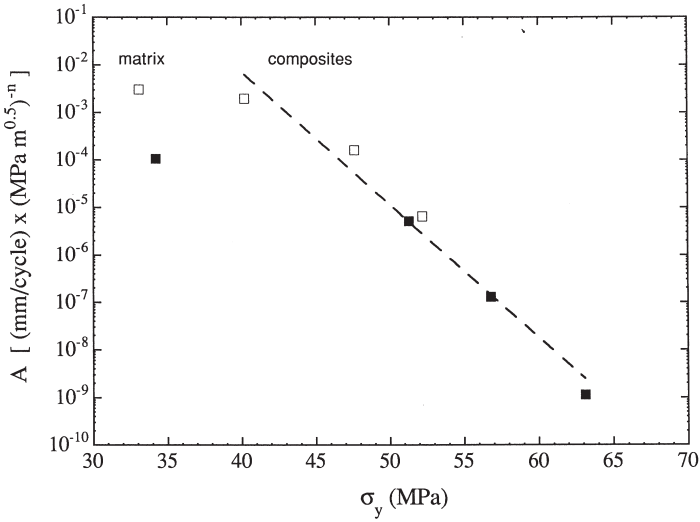

Figure 8. *Pre-exponential* A *coefficient of the Paris-Erdogan equation as a function of tensile yield strength* σ_y*, for fatigue tests performed at a mean load of 1200 N, frequency 1 Hz, minimum to maximum load ratio* R = *0.4. Symbols as follows: (■)* L *direction and (□)* T *direction.*

EFFECT OF FREQUENCY

During the past years a number of studies have been published on the effect of test frequency on FCP rate in engineering thermoplastics, and the results of such studies are most striking [3]. In particular in the range from 0.1 to 100 Hz the FCP resistance of several polymers such as polystyrene [34], poly(phenylene oxide) [34], poly(methyl methacrylate) [35], poly(vinyl chloride) [36], nylon-6 and nylon-6,6 [16], showed a significant improvement with increasing frequency. On the contrary, some other polymers such as polycarbonate [37], and poly(vinylidene fluoride) [38] showed a very slight worsening of FCP rate with increasing test frequency. Concerning the frequency effect on the FCP behavior of short fiber reinforced polymers, limited experimental information exists [8,10,17,39].

Experimental data regarding the effect of test frequency on the FCP growth rate are reported in Figures 9 and 10 for pure and SGF reinforced PP, respectively. For all the materials considered in the present study, a strong decrease of the FCP rate is observed as the test frequency increases.

Hertzberg et al. [34] suggested that during an FCP experiment the overall crack extension rate, $(da/dN)_{total}$, could be considered as the summation of a pure fatigue component, $(da/dN)_{fatigue}$, and a pure creep component $(da/dN)_{creep}$, i.e.:

$$\left(\frac{da}{dN}\right)_{total} = \left(\frac{da}{dN}\right)_{fatigue} + \left(\frac{da}{dN}\right)_{creep} \tag{7}$$

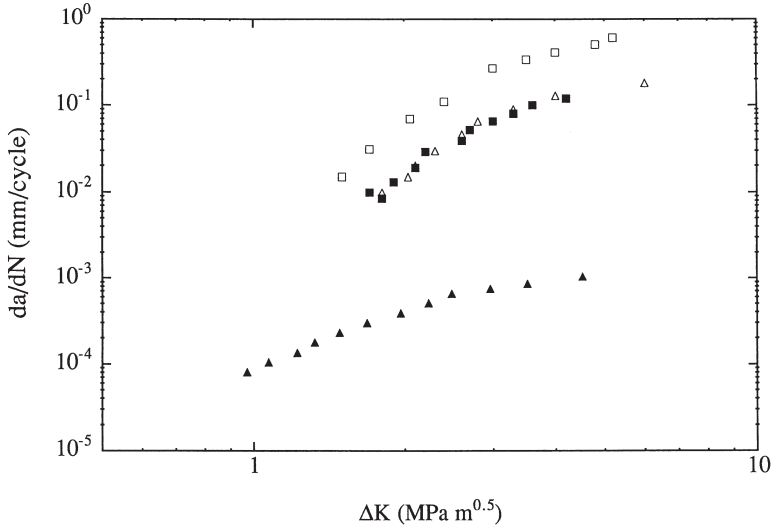

Figure 9. da/dN *vs.* ΔK *curves for the pure PP matrix tested at a mean load of 1200 N, minimum to maximum load ratio* R = *0.4. Symbols as follows: (▲)* L *direction, frequency = 1 Hz; (■)* L *direction, frequency = 0.1 Hz; (△)* T *direction, frequency = 1 Hz; and (□)* T *direction frequency = 0.1 Hz.*

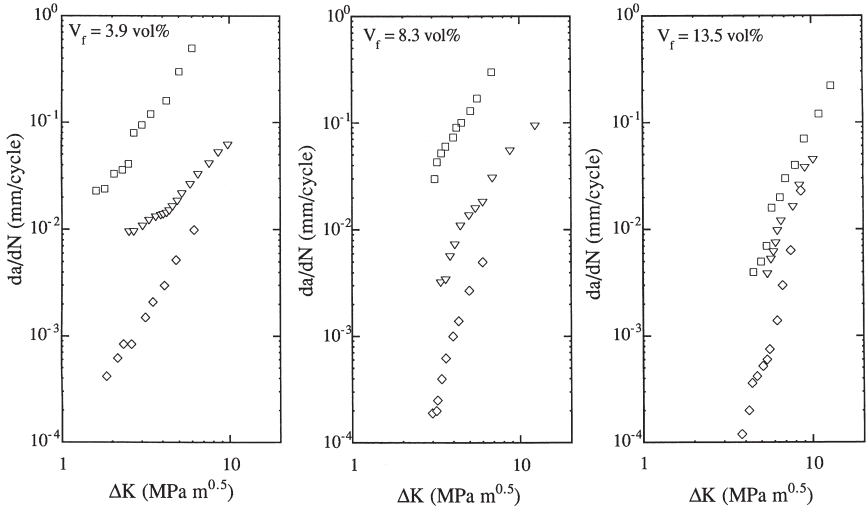

Figure 10. da/dN *vs.* ΔK *curves for T-samples of composites tested at a mean load of 1200 N, minimum to maximum load ratio* R = *0.4. Symbols as follows: (□) frequency = 0.1 Hz; (▽) frequency = 1 Hz; and (◇) frequency = 10 Hz.*

More recently, Wyzgoski and Novak [16] proposed to rearrange Equation (7) as follows:

$$\left(\frac{da}{dN}\right)_{total} = \left(\frac{da}{dN}\right)_{fatigue} + \left(\frac{da}{dt}\right)_{creep} \frac{dt}{dN} \tag{8}$$

where dt/dN is the time period, P, of the cyclic oscillation, which is also equal to the inverse of the frequency ($P = 1/\nu$). This dependence is illustrated in Figure 11, where the crack growth rate per cycle at a fixed level of ΔK is expressed as a function of the time period for various T-samples. According to Equation (7), the intercept of the linear regression represents the crack growth rate contribution due to true fatigue while the slope represents a crack speed due to the contribution of the viscoelastic creep. This procedure can be repeated in order to obtain the creep component of the crack speed at various ΔK values. ΔK is related to the mean applied stress intensity factor, K_{mean}, through the following relationship:

$$K_{mean} = \frac{1+R}{2(1-R)} \Delta K \tag{9}$$

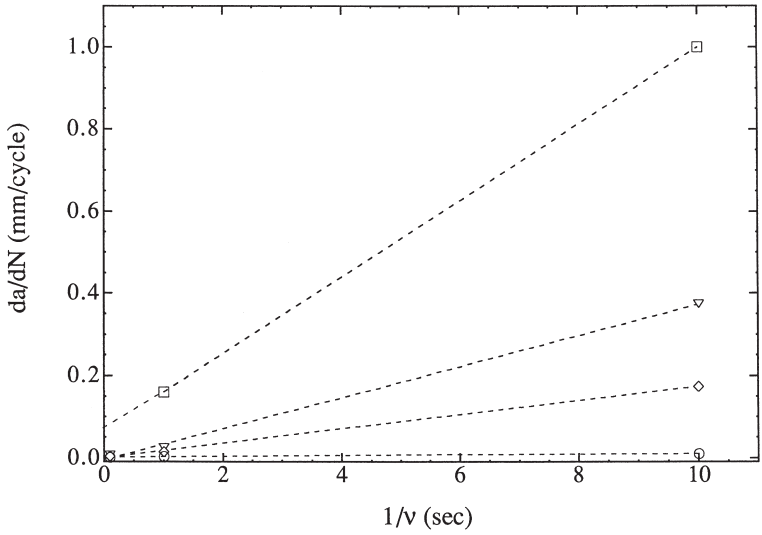

Figure 11. *FCP rate for T-samples evaluated at a constant ΔK value of 5.5 MPa $m^{0.5}$ vs. the fatigue time period (1/ν) for materials with (□) 0 vol%, (▽) 3.9 vol%, (◇) 8.3 vol%, (○) 13.5 vol% of short glass fibers.*

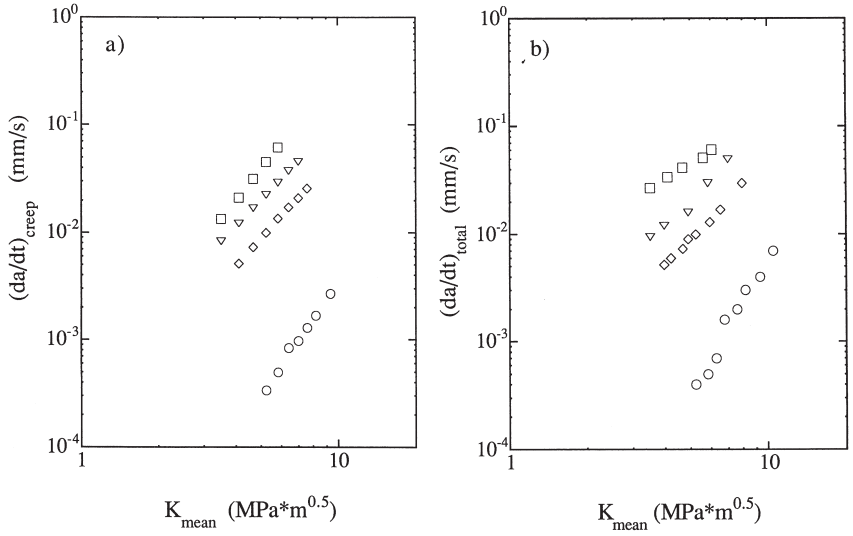

Figure 12. *(a) Creep component, (*$da/dt)_{creep}$ *and (b) experimental total value at a test frequency of 0.1 Hz, (*$da/dt)_{total}$*, of the crack speed as a function of the mean applied stress intensity factor,* K_{mean} *for materials with (□) 0 vol%, (▽) 3.9 vol%, (◇) 8.3 vol% and (○) 13.5 vol% of short glass fibers.*

where R is the minimum to maximum load ratio. As reported in Figure 12(a), it is possible to represent the Log $(da/dt)_{creep}$ component as a function of Log (K_{mean}) with a linear relationship for all the materials examined. In other words the creep component can be reasonably well represented by a Paris-like equation [40] in the form:

$$\frac{da}{dt} = BK_{mean}^{m} \tag{10}$$

which is usually employed for describing crack growth speed under static loads. For sake of comparison, in Figure 12(b) are reported the experimental $(da/dt)_{total}$ values obtained at the test frequency of 0.1 Hz as a function of the K_{mean}. By comparing Figures 12(a) and 12(b) it clearly comes out that, at least at the lowest frequency of 0.1 Hz, most of the crack growth can be attributed to a creep process. As it can be observed from Figure 11 and previously reported in Reference [10], the creep component during the FCP process in a cycle is less and less important as the fiber volume fraction and the test frequency increase. Moreover it is worth pointing out that, as the authors observed in a previous work [10], hysteric heating at the crack tip may occur, particularly at high frequency and low fiber volume fraction. For these cases it is consequently reasonable to hypothesize a crack propagation under non-isothermal conditions.

EFFECT OF MEAN LOAD

Even if a number of studies have been conducted to evaluate the effect of mean stress on the FCP rate in unfilled polymers, the results are quite controversial [3]. Some polymers like poly(methyl methacrylate), poly(vinyl chloride), polystyrene, poly(vinylidene fluoride), epoxy, nylon-66, exhibit an increase in crack growth at fixed ΔK level with increasing the mean load, while other polymers like polycarbonate, ABS, polysulphone, poly(phenylene oxide)/high-impact-polystyrene, low density polyethylene, exhibit lower growth rates as the mean load is increased. Moreover no data are currently available on the effects of the mean stress level on the FCP behavior of SGF reinforced PP.

The effect of the applied mean load on the FCP behavior at 1 Hz was investigated on L-samples of composites reinforced with 13.5 vol% of SGF, the load amplitude being constant (600 N). As reported in Figure 13, as the mean load (and consequently R) decreases the FCP curves shift toward lower ΔK values, or in other words the crack growth rate at a fixed ΔK is reduced. This effect can be further analyzed by looking at the pre-exponential factor, A, and the slope, n, of the Paris-Erdogan equation, as a function of the mean applied load (see Figure 14). Extrapolation to zero mean load gives an estimation of the FCP behavior under pure fatigue condition. In our case the linear extrapolation leads to estimate $A = 1.37*10^{-6}$ [(mm/cycle) × (MPa $m^{0.5})^n$] and $n = 0.6$.

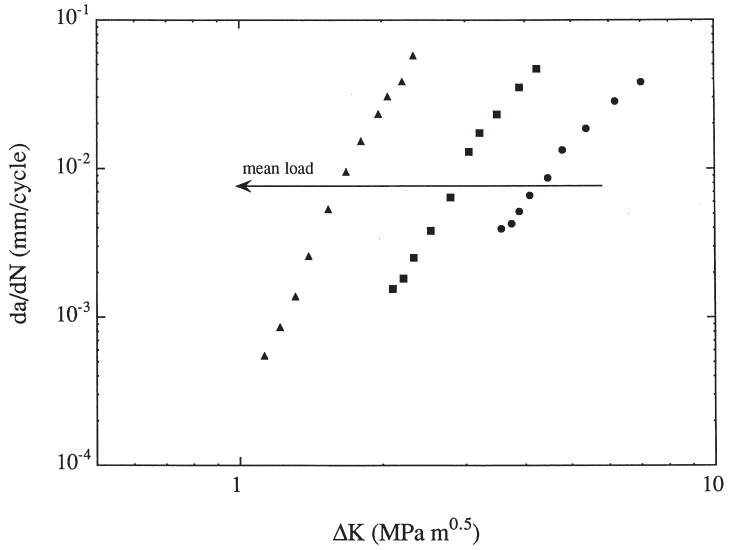

Figure 13. da/dN *vs.* ΔK *curves for L-samples of composites reinforced with 13.5 vol% of short glass fibers during FCP tests at a constant load amplitude of 600 N. Symbols as follows: (●) mean load = 800 N (*R *= 0.46); (■) mean load = 1050 N (*R *= 0.56); and (▲) mean load = 1440 N (*R *= 0.66).*

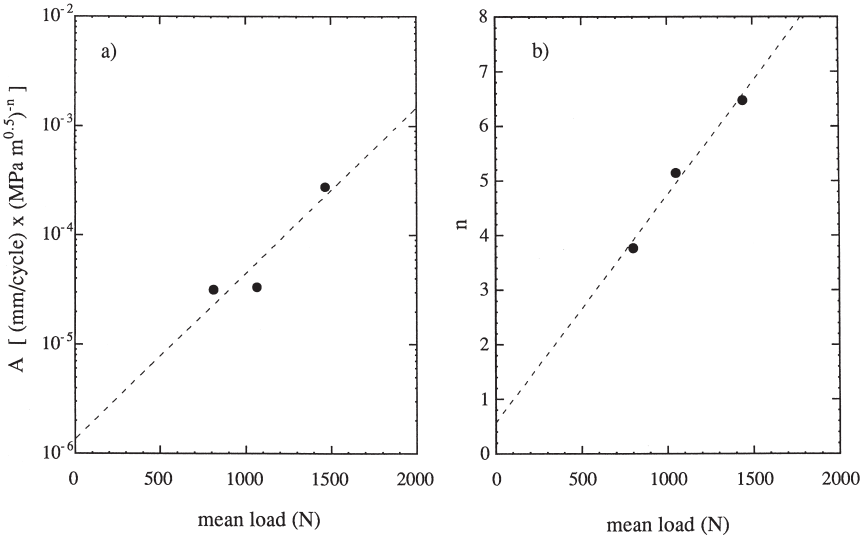

Figure 14. *(a)* A *and (b)* n *coefficients of the Paris-Erdogan equation as a function of the mean applied load for FCP tests performed on L-samples of composites reinforced with 13.5 vol% of short glass fibers at a constant load amplitude of 600 N.*

CONCLUSIONS

In conclusion, it can be stated that the FCP rate in unfilled and short glass fiber reinforced polypropylene is highly dependent on the crack propagation direction, with lower values for crack propagating transversely to the melt flow direction in the molded plaques. In particular for the composite materials the logarithm of the pre-exponential factor of the Paris-Erdogan equation appears to be linearly related to the material yield strength.

For all the materials under investigation the fatigue crack growth rate per cycle strongly increases as the test frequency decreases and the mean applied load increases. Analysis of data obtained at various frequencies and applied mean loads suggests that crack propagation under cyclic loading conditions is mostly due to viscoelastic creep processes at the crack tip.

ACKNOWLEDGEMENTS

This work was partially supported by Consiglio Nazionale delle Ricerche, CNR, Rome. Montell Polyolefins SpA (Ferrara, Italy) is kindly acknowledged for the provision of the materials. The authors would like to thank Dr. F. Fedrizzi and Dr. F. Martinatti for their contribution.

REFERENCES

1. Dufton, P. 1992. "Use of PP in the automotive industry," in *Proceedings of Polypropylene in Automotive Industry Conference,* The Patrick Collection, Birmingham, UK, pp. 1–12.
2. Karger-Kocsis, J. 1995. "Microstructural aspects of fracture in polypropylene and its filled, chopped fiber and fiber mat reinforced composites," in J. Karger-Kocsis (ed.), *Polypropylene Structure, Blends and Composites. Volume 3 Composites,* London: Chapman & Hall, pp. 142–201.
3. Hertzberg, R.W. and J.A. Manson. 1980. *Fatigue of Engineering Plastics,* New York: Academic Press.
4. Karger-Kocsis, J. and K. Friedrich. 1989. "Effect of skin-core morphology on fatigue crack propagation in injection moulded polypropylene homopolymer," *Int. J. Fracture,* 11: 161–168.
5. Karger-Kocsis, J., K. Friedrich and R.S. Bailey. 1991. "Fatigue crack propagation in short and long glass fiber reinforced injection-molded polypropylene composites," *Adv. Composite Materials,* 1: 103–121.
6. Karger-Kocsis, J. 1991. "Microstructural aspects of the fatigue crack growth in polypropylene and its chopped glass fiber reinforced composites," *J. Polymer Engineering,* 10: 97–121.
7. Karger-Kocsis, J. 1991. "Structure and fracture mechanics of injection-molded composites," in S.M. Lee (ed.) *International Encyclopedia of Composites,* vol. 5, New York: VCII Publ., pp. 337–356.
8. Fedrizzi, F., F. Martinatti and T. Ricco. 1995. "Fatigue fracture of polypropylene/glass fibre composites," in *3rd International Conference on Deformation and Fracture of Composites,* University of Surrey, Guildford, UK, pp. 362–367.
9. Ferreira, J.A.M., J.D.M. Costa and M.O.W. Richardson. 1997. "Effect of notch and test conditions on the fatigue of a glass-fibre-reinforced polypropylene composite," *Composites Science & Technology,* 57: 1243–1248.
10. Pegoretti, A. and T. Ricco. 1999. "Fatigue crack propagation in polypropylene reinforced with short glass fibres," *Composites Science & Technology,* 59: 1055–1062.
11. Paris, P.C. and F. Erdogan. 1963. "A critical analysis of crack propagation laws," *J. Basic Eng. Trans.,* 85: 528–537.
12. Goettler, L.A. 1986. "The effects of processing variables on the mechanical properties of reinforced thermoplastics," in D.W. Clegg and A.A. Collyer (eds.) *Mechanical Properties of Reinforced Thermoplastics,* London: Elsevier Applied Science Publishers, pp. 151–204.
13. Lang, R.W., J.A. Manson and R.W. Hertzberg. 1987. "Mechanisms of fatigue fracture in short glass fibre-reinforced polymers," *J. Mater. Science,* 22: 4015–4030.
14. Karger-Kocsis, J. and K. Friedrich. 1988. "Fatigue crack propagation in short and long fibre-reinforced injection-moulded PA 66 composites," *Composites,* 19: 105–114.
15. Martin, D.C., G.E. Novak and M.G. Wyzgoski. 1989. "Fatigue fracture of reaction injection molded (RIM) nylon composites," *J. Applied Polymer Science,* 37: 3029–3056.
16. Wyzgoski, M.G., G.E. Novak and D.L. Simon. 1990. "Fatigue fracture of nylon polymers. Part 1 Effect of frequency," *J. Mater. Science,* 25: 4501–4510.
17. Wyzgoski, M.G. and G.E. Novak. 1991. "Fatigue fracture of nylon polymers. Part 2 Effect of glass-fibre reinforcement," *J. Mater. Science,* 26: 6314–6324.
18. Karger-Kocsis, J. 1990. "Effects of processing induced microstructure on the fatigue crack propagation of unfilled and short fibre-reinforced PA-6," *Composites,* 21: 243–254.
19. Wyzgoski, M.G. and G.E. Novak. 1994. "Direct measurement of strain energy release rates during fatigue fracture of reinforced nylon 66," *International Conference Yield, Deformation and Fracture,* Cambridge, UK, pp. 39/1–39/4.
20. Darlington, M.W. 1991. "Short fibre reinforced thermoplastics: properties and design, in A.H. Cardon and G. Verchery (eds.) *Durability of Polymer Based Composite Systems for Structural Applications,* London: Elsevier Science Publisher, pp. 80–98.

21. Friedrich, K., R. Walter, H. Voss and J. Karger-Kocsis. 1986. "Effect of short fibre reinforcement on the fatigue crack propagation and fracture of PEEK-matrix composites," *Composites,* 17: 205–216.
22. Evans, W.J., D.H. Isaac and K.S. Saib. 1996. "The effect of short carbon fibre reinforcement on fatigue crack growth in PEEK," *Composites Part A,* 27A: 547–554.
23. Voss, H. and J. Karger-Kocsis. 1988. "Fatigue crack propagation in glass-fibre and glass-sphere filled PBT composites," *Int. J. Fatigue,* 1: 3–11.
24. Voss, H. and R. Walter. 1985. Fracture and fatigue of short glass-fibre reinforced polyethersulphone composites," *J. Mat. Science Letter,* 4: 1174–1177.
25. Voss, H. and K. Friedrich. 1986. "Fracture and fatigue of short glass fibre reinforced PTFE composites," *J. Mat. Science Letter,* 5: 569–572.
26. Janimak, J.J., S.Z.D. Cheng, A. Zhang and E.T. Hsieh. 1992. "Isotacticity effect on crystallization and melting in polypropylene fractions: 3. Overall crystallization and melting behaviour," *Polymer,* 33: 728–735.
27. ASTM D 5045, 1993. "Standard test methods for plane-strain fracture toughness and strain energy release rate of plastic materials," Annual Book of ASTM Standard, 08.03.
28. Broek, D. 1987. *Elementary Engineering Fracture Mechanics.* Dordrecht: Martinus Nijhoff Publishers, p. 85.
29. Agarwal, D.B. and J.L. Broutman. 1990. *Analysis and Performance of Fiber Composites. Second edition.* New York: John Wiley & Sons, p. 131.
30. Kardos, J.L. 1990. "Mechanical properties of polymeric composite materials," in E. Baer, A. Moet (eds.) *High Performance Polymers,* Munich: Hanser Publishers, pp. 199–251.
31. Karger-Kocsis, J. 1989. "Microstructure and fracture mechanical performance of short-fibre reinforced thermoplastics," in K. Friedrich (ed.) *Application of Fracture Mechanics to Composite Materials,* Amsterdam: Elsevier Science Publishers, pp. 189–247.
32. Vu-Khanh, T. and B. Fisa. 1986. "Impact fracture of glass-flake reinforced polypropylene," *Polymer Composites,* 7: 375–382.
33. Darlington, M.W. 1991. "Short fibre reinforced thermoplastics: properties and design," in A.H. Cardon and G. Verchery (eds.) *Durability of Polymer Based Composite Systems for Structural Applications,* London: Elsevier Science Publisher, pp. 80–98.
34. Hertzberg, R.W., J.A. Manson and M.D. Skibo. 1975. "Frequency sensitivity of fatigue processes in polymeric solids," *Polymer Engineering and Science,* 15: 252–260.
35. Cheng, W.M., G.A. Miller, J.A. Manson, R.W. Hertzberg and L.H. Sperling. 1990. "Mechanical behaviour of poly(methyl methacrylate). Part 2 The temperature and frequency effects on the fatigue crack propagation behaviour," *J. Mater. Science,* 25: 1924–1930.
36. Hertzberg, R.W. and J.A. Manson. 1973. "Micromechanisms of fatigue-crack advance in PVC," *J. Mater. Science,* 8: 1554–1558.
37. Arad, S., J.C. Radon and L.E. Culver. 1972. "Growth of fatigue cracks in polycarbonate," *Polymer Engineering and Science,* 12: 193–198.
38. Hertzberg, R.W., J.A. Manson and W.C. Wu. 1973. "Structure of polymers and fatigue crack propagation," ASTM STP 536: 391–403.
39. Lang, R.W., J.A. Manson and R.W. Hertzberg. 1983. "Fatigue crack propagation in short-glass fiber-reinforced nylon 6.6: effect of frequency," in J.C. Seferis and L. Nicolais (eds.) *The Role of the Polymeric Matrix in the Processing and Structural Properties of Composite Materials,* New York: Plenum, pp. 377–396.
40. Williams, J.G. 1984. *Fracture Mechanics of Polymers,* West Sussex, England: Ellis Horwood Ltd., p. 176.